

# Periodic Asynchrony: An Effective Method for Accelerating Reinforcement Learning for Large Language Models

Jian Lu

Big Data & AI Lab, Industrial and Commercial Bank of China (ICBC)

janelu@live.cn

## Abstract

Since the introduction of the GRPO algorithm, reinforcement learning (RL) has attracted increasing attention, with growing efforts to reproduce and apply it. However, training efficiency remains a critical challenge. In mainstream RL frameworks, inference and training are typically deployed on the same devices. While this approach reduces costs through resource consolidation, its synchronous execution imposes a computational coupling that prevents concurrent inference and training. In this study, we are returning to the strategy of separating inference and training deployment, and by introducing improvements in the data loader, we transform the conventional synchronous architecture into a periodically asynchronous framework, which allows for demand-driven, independent, and elastic scaling of each component, while the accuracy of the algorithm remains completely equivalent to the synchronization method, with both belonging to the on-policy strategy. It is worth emphasizing that we apply a unified tri-model architecture in the training phase, and we also proposed a shared-prompt attention mask to reduce repetitive computation. In practice, these works have achieved at least a threefold overall performance improvement in RL training on NPU platforms, indicating its potential for widespread application.

## 1 Introduction

Reinforcement learning (RL) has re-emerged as a key technique for post-training and aligning large language models (LLMs). Following the introduction of GRPO by DeepSeek-R1 [Guo *et al.*, 2025], RL has demonstrated strong potential in improving reasoning capabilities, sparking growing interest in efficient RL pipelines across academia and industry.

Despite these advances, RL for LLMs still faces severe efficiency challenges. The training pipeline requires multiple models in the forward pass—the policy model, old-policy model, and reference model, and in some cases a value and reward model [Schulman *et al.*, 2017]—leading to substantial computational overhead. Moreover, each training step

typically depends on generating large numbers of chain-of-thought (CoT) [Wei *et al.*, 2022] trajectories using the latest policy weights, further increasing inference cost and memory usage.

To improve efficiency, early systems such as DeepSpeed-Chat [Yao *et al.*, 2023] relied on ZeRO-based distributed training, where the policy model handled inference directly, resulting in limited throughput. Later approaches decoupled training and inference, leveraging inference engines like vLLM [Kwon *et al.*, 2023] to accelerate rollout generation, as demonstrated by Open-R1 [Hugging Face, 2025]. Industry systems such as OpenRLHF [Hu *et al.*, 2024] push this further through training–inference co-location, although task switching still prevents full concurrency and independent scalability. Meanwhile, frameworks such as MindSpeed-RL [Feng *et al.*, 2025] and VERL [Sheng *et al.*, 2024] improve the training side through Megatron-style 3D parallelism [Shoeybi *et al.*, 2019].

Motivated by these limitations, we revisit the training–inference separation strategy and introduce a synchronous framework enhanced with new system-level optimizations. Our design uses a Megatron-style 3D parallel backbone and adds a background producer process that continuously dispatches prompts to inference workers, while the main consumer process retrieves outputs and performs training. Samples from each group are split into micro-batches and trained sequentially, and model weights are synchronized only after the full batch is consumed. This *periodic asynchrony* achieves purely on-policy asynchronous acceleration and is compatible with any on-policy RL algorithm. The decoupled architecture enables flexible scaling of inference workers, avoiding inference bottlenecks, and for GRPO, we further introduce a shared-prompt attention mask to eliminate redundant computation. Experiments show that on a 16-NPU setup training an 8B model with 16k context, our approach delivers over a threefold improvement in end-to-end RL throughput.

## 2 Related Work

Improving the efficiency of reinforcement learning (RL) for large language models (LLMs) has attracted increasing attention across academia and industry. Although synchronous frameworks dominate large-scale RL systems due to their stability, they often underutilize computational resources. To

address this, recent studies explore asynchronous training paradigms that decouple inference from training to enhance throughput and scalability. We review representative efforts, with emphasis on asynchronous RL methods.

An early attempt is Asynchronous RLHF [Noukhovitch *et al.*, 2024], which decouples generation and learning so that new sample generation and old-sample training proceed in parallel. Its key idea is online but off-policy RLHF, updating models with samples from previous iterations. While effective, it remains a typical off-policy strategy and is less suitable for strictly on-policy algorithms such as GRPO, especially in long-context settings.

Most recently, AReaL [Fu *et al.*, 2025] advanced the application of asynchronous RL to LLM reasoning tasks by fully decoupling generation from training. It introduces a parameter  $\eta$  to control data staleness, enabling better handling of delayed samples. To better handle delayed samples, it incorporates a staleness-enhanced PPO variant, effectively modifying the on-policy paradigm to tolerate partially off-policy data. Additionally, its training start time depends on the completion of the first inference batch. In a similar vein, ROLL Flash [Lu *et al.*, 2025], also recently introduced, shares conceptual similarities with AReaL. Like AReaL, it decouples training from inference and controls the proportion of off-policy data through an async ratio. Both AReaL and ROLL Flash are off-policy asynchronous frameworks that improve training efficiency but require modifications to standard on-policy RL algorithms to handle data bias. This design trades a small portion of data originally intended for strictly on-policy training to avoid inference-service blocking, effectively shifting it toward off-policy learning. Although their experiments demonstrate the effectiveness of this biased setup, whether it generalizes across all RL algorithms and data regimes remains theoretically unproven.

In contrast, our method takes a different perspective with several innovations:

- **Algorithm-decoupled periodic asynchrony** enabling purely on-policy asynchronous acceleration without sacrificing stability.
- **Decoupling prompt-level inference *production* from sample-level training *consumption***, maximizing overlap between the two.
- A **shared-prompt mask** for efficient reuse of forward/backward computation on prompt tokens.
- A **distribution-consistent design** across policy, old-policy, and reference models, simplifying scaling and system structure.
- **Independent scalability** of inference and training instances, preventing bottlenecks in either component.

Together, these designs enable efficient long-context training with substantially fewer computational resources. All components are implemented in project release v5.0.5 (September 5, 2025): <https://github.com/janelu9/EasyLLM>.

### 3 Background

#### Training RL with Micro-Batching

It is well known that when using distributed architectures for large-scale model pre-training or fine-tuning, one typically does not train on an entire batch and immediately update the model parameters with the resulting gradients, as is common in single-GPU training for small models. A full batch usually contains hundreds or even thousands of samples, and directly processing it in large-model training can easily lead to GPU out-of-memory (OOM) errors. Instead, the batch is divided into multiple micro-batches, each containing only one or two samples. These micro-batches are processed sequentially, with a buffer tensor used to accumulate the gradients from each micro-step. The accumulated gradients are applied to update the model parameters only after all micro-batches within the batch have been processed. In practice, these two training strategies are mathematically equivalent.

The gradient update rule for full-batch training is:

$$W_{t+1} = W_t - \alpha \frac{1}{N} \sum_{n=1}^N g_n, \quad (1)$$

and for micro-batch training, after accumulating gradients over all micro-batches, the update rule is:

$$W_{t+1} = W_t - \alpha \frac{1}{M} \sum_{i=1}^M \frac{1}{m} \sum_{j=1}^m g_{i,j}, \quad (2)$$

where  $M$  is the total number of micro-batches,  $m$  is the number of samples in each micro-batch, and  $g_{i,j}$  is the gradient of the  $j$ -th sample in the  $i$ -th micro-batch. This demonstrates that both training strategies are mathematically equivalent, but micro-batching offers significant memory savings.

Consider the objective function of GRPO for generating responses from a single prompt:

$$J_{\text{GRPO}}(\theta) = \frac{1}{G} \sum_{i=1}^G \left( L_i(\pi_\theta \| \pi_{\text{old}}, A_i) - \beta D_{KL}^i(\pi_\theta \| \pi_{\text{ref}}) \right). \quad (3)$$

The PPO-style clipped advantage term can be split into two lines as follows:

$$L_i(\pi_\theta \| \pi_{\text{old}}, A_i) = \min \left( \frac{\pi_\theta(o_i|q)}{\pi_{\theta_{\text{old}}}(o_i|q)} A_i, \right. \\ \left. \text{clip} \left( \frac{\pi_\theta(o_i|q)}{\pi_{\theta_{\text{old}}}(o_i|q)}, 1 - \varepsilon, 1 + \varepsilon \right) A_i \right). \quad (4)$$

The KL divergence term is given by:

$$D_{KL}^i(\pi_\theta \| \pi_{\text{ref}}) = \frac{\pi_{\text{ref}}(o_i|q)}{\pi_\theta(o_i|q)} - \log \frac{\pi_{\text{ref}}(o_i|q)}{\pi_\theta(o_i|q)} - 1. \quad (5)$$

For a batch of  $N$  prompts, the objective becomes:

$$\begin{aligned}
J_{\text{batch}} &= \frac{1}{N} \sum_{i=1}^N J_{\text{GRPO}}^i \\
&= \frac{1}{N} \sum_{i=1}^N \frac{1}{G} \sum_{j=1}^G (L_{i,j} - \beta D_{KL}^{i,j}) \\
&= \frac{1}{NG} \sum_{i=1}^{NG} (L_i - \beta D_{KL}^i).
\end{aligned} \tag{6}$$

Define

$$M = \frac{NG}{m}. \tag{7}$$

Then the batch objective can be rewritten using micro-batches:

$$J_{\text{batch}} = \frac{1}{M} \sum_{i=1}^M \frac{1}{m} \sum_{j=1}^m (L_{i,j} - \beta D_{KL}^{i,j}). \tag{8}$$

This demonstrates that reinforcement learning can also be trained using micro-batches. Compared with pre-training or fine-tuning, a batch now contains  $NG$  samples, but GPU memory usage is greatly reduced. Consequently, reinforcement learning can handle sequences as long as those supported during fine-tuning.

## 4 System Design

### 4.1 Unified Tri-Model Architecture

When performing reinforcement learning with large-scale models using different frameworks for inference and training—for instance, vLLM for inference and Megatron for training—the process generally involves three main steps:

1. Synchronize the weights of the policy model with the inference engine.
2. The inference engine retrieves prompts from the dataloader and generates responses. A reward module evaluates these responses based on the corresponding prompts, distinguishing high-quality outputs from lower-quality ones.
3. The generated samples and their associated scores are then sent to the training engine, which computes the loss and performs backpropagation to update the policy model parameters.

For the third step, mainstream reinforcement learning systems typically require the computation of three types of logits in the forward pass: policy, old policy, and reference. These models share the same architecture, differing only in their weights. In this work, the training phase is implemented using a Megatron-like architecture, where a complete policy model is distributed across multiple computational units according to tensor parallelism and pipeline parallelism scales. During the forward computation of the old policy and reference models, each sub-network managed by the policy model is replicated twice across all computational units—once for computing the old policy logits and once for computing the

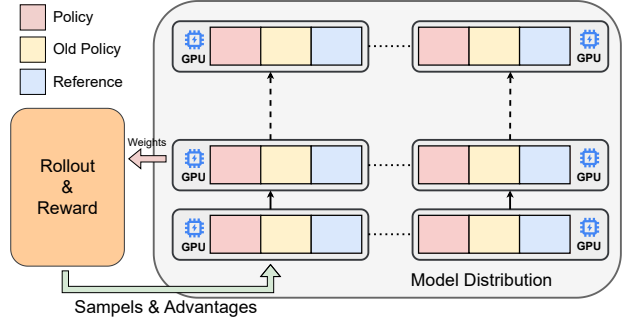


Figure 1: Triple Models with Shared Distribution.

reference logits. The reference network retains the original model weights, while the old policy network holds weights delayed by one training step relative to the policy model.

The overall architecture of the reinforcement learning system constructed in this work is illustrated in Figure 1. The three types of models share an identical architecture and are distributed in the same parallel layout. This design allows their logits to be computed simultaneously without requiring any additional topology for the reference model. The inference stage, in contrast, is handled by an independent inference engine such as vLLM. Before training each batch, the weights of the policy model are synchronized to all inference engines. The inference engines then receive prompts from the dataset, generate responses, and return them for scoring. Each scored response is concatenated with its corresponding prompt to form a training sample, which is fed into all three models for forward computation. In a single micro-step, we obtain the logits from the policy, old policy, and reference models simultaneously. After all samples in a batch complete their forward passes—and before the policy model's weights are updated—its current weights are moved into the old policy model's `state_dict`.

### 4.2 Shared-Prompt Attention

In reinforcement learning training, each group of samples shares the same prompt. In fact, during micro-batch training, if the micro-batch size is greater than 1, the prompt can be reused. When the prompt contains many tokens while the generated responses are relatively short, reusing the prompt can significantly reduce redundant computation and GPU memory usage, thereby improving overall training efficiency.

Compared with standard training, when adopting the shared-prompt approach, the following modifications are made:

1. Concatenate the shared prompt with the token IDs of multiple responses. The corresponding labels are concatenated accordingly, while the prompt portion is excluded from the labels.

$$\begin{cases} x = [x_p, x_{r_1}, x_{r_2}] \\ y = [y_{r_1}, y_{r_2}] \end{cases} \tag{9}$$

In this formulation,  $x_p$  denotes the token IDs of the shared prompt, and  $x_{r_1}, x_{r_2}$  correspond to the tokens of the individual responses.

2. Rearrange the position indices such that each response starts immediately after the prompt, ensuring positional continuity with the shared prompt.

$$p = (0, 1, \dots, |x_p| - 1, |x_p|, \dots, |x_p| + |x_{r_1}| - 1, |x_p|, \dots, |x_p| + |x_{r_2}| - 1) \quad (10)$$

Here, the notation  $|\cdot|$  indicates sequence length.

3. In the attention module, a shared-prompt mask (Figure 2) is used instead of the standard causal mask. This design restricts each response token to attend only to the shared prompt, preventing information leakage across responses.

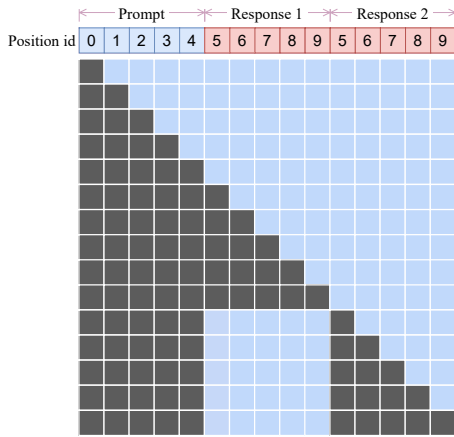


Figure 2: Shared-prompt attention mask.

4. For probability computation, the prompt tokens are discarded and the loss is computed only over the response tokens:

$$\pi = -\text{CrossEntropy}(\hat{y}_{|x_p|:|x|}, y), \quad (11)$$

where  $\hat{y}_{|x_p|:|x|}$  represents the predicted logits of the response tokens.

All other aspects remain the same as in standard training. This grouped micro-batch approach is generally more computationally efficient than simply concatenating micro-batches along the first axis, because the prompt tokens only need to be computed once, and padding is not required for shorter samples within a micro-batch. The advantage becomes especially pronounced when the prompt is long and the responses are relatively short.

### 4.3 Periodic Asynchronous Reinforcement Learning

Asynchronous execution of inference and training is a key factor in accelerating reinforcement learning systems with a separated training-inference architecture. In such asynchronous systems, the critical aspect is minimizing the time the training engine waits for the rollout workers to return generated samples, i.e., the startup latency. In this work, we propose a simple approach that introduces a temporary data

generator between the data loader and the trainer. This design transforms on-policy reinforcement learning from synchronous to asynchronous execution, significantly improving training efficiency without requiring any modifications to the underlying reinforcement learning algorithm.

The reinforcement learning workflow incorporating the temporary sample generator is illustrated in Figure 3. It follows a typical *producer-consumer* pattern and consists of four main components:

1. **Data source**, which is the original data loader.
2. **Temporary data generator**, the additional component introduced in this work, which includes a background thread acting as a producer and a queue shared with the main process.
3. **Inference service**, responsible for receiving prompts and generating responses.
4. **Trainer**, which consumes the samples from the queue for training.

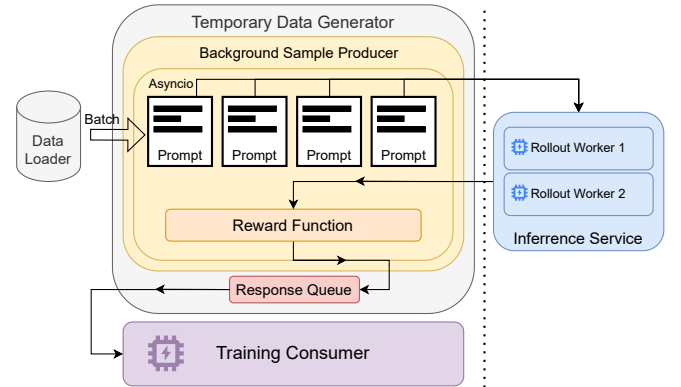


Figure 3: Operational Mechanism of the Asynchronous System.

The core of our asynchronous design lies in the operation of the temporary generator. Within the temporary generator, a batch of prompts required for one training step is first retrieved from the standard data loader. A background thread is then launched to act as a *producer*. Inside this thread, a coroutine is used to concurrently and evenly dispatch the entire batch of prompts to multiple inference instances within the inference service. Upon receiving a large number of requests, the inference instances efficiently generate responses through continuous batching and return the completed responses back to the coroutine.

To fully exploit coroutine-level parallelism, the reward function is integrated directly into the coroutine. Each response returned by an inference instance is immediately scored, and once both inference and evaluation for a coroutine's assignment are finished, the resulting responses and reward scores are placed into a queue shared with the main process. This queue serves as a buffer that temporarily stores the generated responses from inference service.

The main process, acting as the *consumer*, continuously retrieves completed samples from the queue and feeds them

to the three models for training. Under this design, the start time of training is determined by the earliest completed sample among all prompts in the batch. Once all prompts in the batch have been processed, the inference service enters an idle state until the training step finishes and the updated policy weights are synchronized back to the rollout workers. Only then does the next training cycle begin. Therefore, we refer to this design as **periodic asynchrony**.

**Algorithm 1** Periodic Asynchronous Reinforcement Learning Algorithm

**Input:** Dataloader  $D$ , training iterations  $T$ , batch size  $B$   
**Output:** Trained policy model

```

1: Initialize shared queue  $Q$  and gradient accumulator  $O$ 
2: for  $t = 1$  to  $T$  do
3:   Synchronize policy model weights to the rollout workers
4:   Retrieve prompts  $P = \{p_1, \dots, p_B\}$  from  $D$ 
5:   Producer thread:
6:     Create  $B$  concurrent coroutine tasks
7:     Run in parallel for each  $i = 1, \dots, B$ :
8:        $r_i \leftarrow \text{InferenceService}(p_i)$ 
9:        $a_i \leftarrow \text{RewardFunction}(r_i)$ 
10:      Enqueue  $(a_i, r_i)$  into  $Q$ 
11:       $O \leftarrow 0$ 
12:       $\text{consumed\_count} \leftarrow 0$ 
13:      while  $\text{consumed\_count} < B$  do
14:         $(a_i, r_i) \leftarrow \text{Dequeue}(Q)$ 
15:         $s_i \leftarrow \text{ProcessSample}(p_i, r_i)$ 
16:        Compute loss  $L(s_i)$  then backward
17:         $O \leftarrow O + \nabla L(s_i)$ 
18:         $\text{consumed\_count} \leftarrow \text{consumed\_count} + 1$ 
19:      end while
20:      Move policy's weights into old-policy's modules
21:      Update policy's weights using gradient  $O$ 
22:    end for

```

In this way, the system constitutes a fully on-policy asynchronous reinforcement learning framework that remains decoupled from the underlying RL algorithm, meaning that no algorithmic modifications are required to ensure correct operation within this asynchronous setup. Algorithm 1 is the pseudocode for the asynchronous reinforcement learning system proposed in this paper.

Figure 4a and Figure 4b illustrate the differences between the asynchronous training system studied in this paper and a synchronous training system. It is evident that in a synchronous system, the training process must wait for all prompts to be processed by the inference service. If the batch size is large, multiple inference batches may be required to complete all the prompts. The startup time for training is determined by the inference batches and the sum of the inference times of the slowest samples in each batch. Assuming the inference engine has a batch size of  $m$  and the prompts of one training batch are divided into  $n$  inference batches, the training startup time can be expressed as:

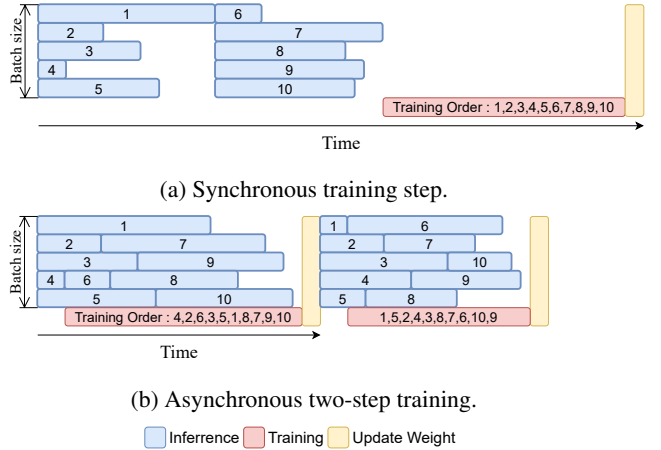


Figure 4: Comparison of synchronous vs. asynchronous training.

$$T_{\text{sync}} = \sum_{j=0}^n \max \left\{ t_i^j \mid i \in \{0, 1, \dots, m\} \right\} \quad (12)$$

Where  $t_i^j$  denotes the time required for the  $i$ -th prompt in the  $j$ -th batch to complete inference. In contrast, for an asynchronous system, the training startup time depends only on the earliest-completed prompt in the first inference batch, which can be expressed as:

$$T_{\text{async}} = \min \left\{ t_i^0 \mid i \in \{0, 1, \dots, m\} \right\} \quad (13)$$

After that, all samples in the batch are trained sequentially in the order in which they enter the queue. It is clear that when inference speed and training speed are well balanced, the sum of their waiting times is minimized, resulting in optimal end-to-end training throughput on a given hardware configuration. The decoupled inference-training architecture naturally enables such balancing by allowing independent configuration of inference and training instances.

Therefore, in theory, when a training batch cannot be processed within a single inference batch, the asynchronous system can achieve more than twice the startup speed of the synchronous system.

## 5 Implementation

Our implementation is built on the **PyTorch** training framework, using a 3D-parallel distributed architecture. We incorporate parts of Megatron-Core v0.8.0 and DeepSpeed v0.17.2 [Rasley *et al.*, 2020]. On the **NPU** platform, we additionally use MindSpeed v2.1.0\_core\_r0.8.0, torch\_npu, and optimized operators such as npu\_fusion\_attention, an accelerated attention kernel supporting custom masks and serving as a counterpart to flash\_attention [Dao, 2023].

For inference, we use **vLLM**, with `ascend_vLLM 0.9.2.rc1` on NPUs. As in fine-tuning, all RL samples are computed at their native sequence lengths for both forward and backward passes without padding, following **dynamic-length training**.

## 6 Experiments

This study conducts comparative experiments on mathematical reasoning tasks, evaluating three reinforcement learning frameworks: MindSpeed-RL, which uses a shared-resource architecture for training and inference; the synchronous reinforcement learning framework implemented in this work under a decoupled training–inference design; and the proposed asynchronous reinforcement learning framework. The main goal is to experimentally compare periodic asynchronous and synchronous training, assess the performance of the proposed system against mainstream synchronous frameworks, and evaluate the scalability of the periodic asynchronous system. The primary evaluation metric is end-to-end training throughput, measured by tokens trained per second per device (TPSPD), calculated as the total number of tokens processed divided by the total elapsed time and the number of devices used. Accuracy metrics are provided for reference to verify algorithm correctness, as no modifications were made to the reinforcement learning algorithm.

Experiments were conducted on **air-cooled** Ascend-910B NPUs, with each node equipped with eight 64 GB NPUs. The intra-node interconnect bandwidth is 196 GB/s, and the inter-node bandwidth is 100 Gb/s.

### 6.1 Model and Environment Configuration

The models compared in this section are Qwen3-8B [Team, 2025] and DeepSeek-R1-Distill-Qwen-32B [DeepSeek-AI, 2025] (since the current version of Mindspeed-RL does not yet support reinforcement learning training for Qwen3-32B, we instead use DeepSeek-R1-Distill-Qwen-32B as the training model.). The training data comes from the publicly available math problem dataset DeepScaler [Luo and others, 2025]. All reinforcement learning experiments use the GRPO algorithm. The accuracy test set is the AIME24 [Zhang and Math-AI, 2024].

Framework	Training Steps	AIME24	Trained Tokens (M)	Training Hours	NPUs	Tokens/Sec/Device
Baseline	0	0.725	0	0	0	–
MindSpeed-RL	100	0.733	706.355	198.942	16	61.641
Sync (ours)	100	0.746	827.306	143.678	16	99.966
Async (ours)	100	0.758	917.609	82.861	16	192.259

Table 1: Accuracy and training efficiency comparison on Qwen3-8B. All frameworks were trained for 100 steps, and training time and token counts were extracted from logs. For our synchronous and asynchronous methods under the training–inference decoupled architecture, 8 NPUs were used for one training instance (TP = 8, PP = 1) and 8 NPUs for four inference instances (TP = 2). MindSpeed-RL used all 16 NPUs for two training instances (TP = 8, PP = 1) and eight inference instances (TP = 2).

Framework	Training Steps	AIME24	Trained Tokens (M)	Training Hours	NPUs	Tokens/Sec/Device
Baseline	0	0.726	0	0	0	–
MindSpeed-RL	20	0.696	107.874	70.647	64	6.627
Async (ours)	20	0.737	123.999	21.453	48	33.449

Table 2: Accuracy and training efficiency comparison on DeepSeek-R1-Distill-Qwen-32B. All frameworks were trained for 20 steps, and training time and token counts were taken from logs. Our asynchronous setup uses 32 NPUs for one training instance (TP = 8, PP = 4) and 16 NPUs for four inference instances (TP = 4). MindSpeed-RL uses all 64 NPUs for two training instances (TP = 8, PP = 4) and 16 inference instances (TP = 4).

### 6.2 Comparison between Asynchronous and Synchronous Training

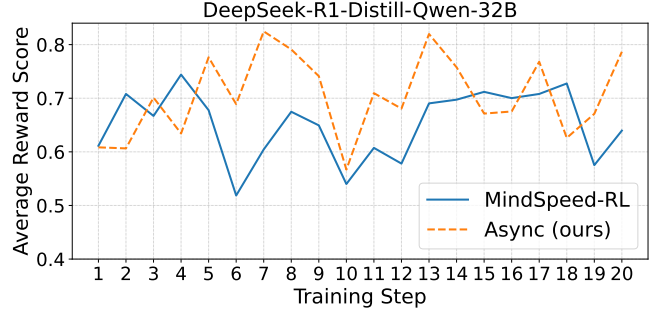
Given that the prompts for the samples are relatively short while the responses are longer, *Shared-Prompt Attention* is disabled in the experiments. In the first set of experiments, Qwen3-8B was used as the training model, with a context length of 16k. As shown in Table 1, in terms of TPSPD, the training speed ratio among the three implementations was **1:1.62:3.12**. The model used in the second set of experiments is DeepSeek-R1-Distill-Qwen-32B, with a context length of 16k, and only two experiments were conducted. As shown in Table 2, the evaluation methodology is identical to that used in the first set of experiments. According to the results, for the 32B-scale model, the ratio of the TPSPD metric between Mindspeed-RL and our asynchronous framework is **1:5.05**.

For accuracy evaluation, we employed a rule-based method where the predicted answer from the policy model is considered correct if it can be accurately extracted and matches the ground-truth answer in the dataset; otherwise, it is deemed incorrect. The tests were conducted using the inference engine `vLLM 0.9.1.rc` with an output length limit of 32k. Each test sample was evaluated 8 times, with inference parameters set to `temperature = 0.7, top_p = 0.95, and top_k = 20`. The results show that the models trained by all three frameworks achieved similar accuracy on the AIME24 benchmark, with any differences falling within the expected range of random fluctuations. This supports the equivalence in performance between the asynchronous and synchronous methods implemented in this study.

We also monitored the reward scores during training for all three frameworks, as shown in Figure 5a. The reward trajectories of our synchronous and asynchronous methods are almost identical, suggesting that the asynchronous approach is computationally equivalent to the synchronous one. Both curves exhibit a slight upward trend, likely because the baseline model was pre-trained on similar data. Figure 5b presents a comparison of reward scores between Mindspeed-RL and



(a) Synchronous vs. Asynchronous.



(b) Mindspeed-RL vs. our Asynchronous.

Figure 5: Training step-wise average reward score comparison.

our asynchronous architecture, and it appears that the trends are generally consistent.

Combining the results of the two experimental groups, we obtain a clear comparative plot of the training speeds, as shown in Figure 6.

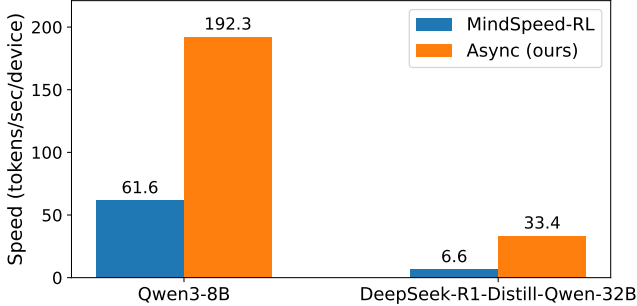


Figure 6: TPSPD: MindSpeed-RL vs. Async (ours).

### 6.3 Asynchronous Scalability Experiments

We also conducted a set of experiments to evaluate the scalability of our framework, using the same configuration as in the first experiment group. The results are shown in Table 3.

Model	NPUs	Training Steps	Tokens/Sec/Device
Qwen3-8B	16	20	188.162
	32	20	171.824
	64	20	163.208

Table 3: Scalability comparison results. TPSPD performance of training Qwen3-8B on 16, 32, and 64 NPUs using our asynchronous framework. The training-to-inference instance ratio is fixed at 1:4.

When expressed in TPS (tokens per second), the results are more intuitively illustrated in Figure 7. Training with 32 NPUs shows a 1.83 $\times$  speedup compared to 16 NPUs, while using 64 NPUs results in a 1.9 $\times$  speedup over 32 NPUs. Overall, the proposed asynchronous reinforcement learning framework demonstrates near-linear scaling in training speed as the number of devices increases.

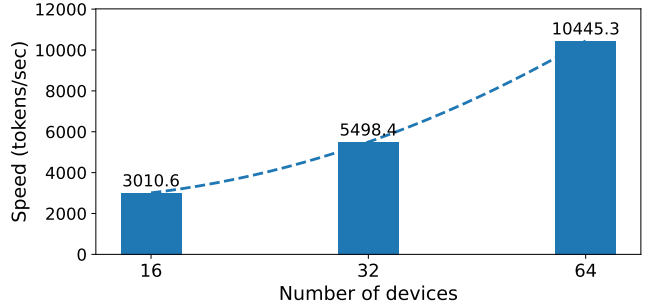


Figure 7: TPS of our framework under different data-parallel scales.

## 7 Conclusion

This paper introduces an asynchronous on-policy reinforcement learning algorithm that maintains the same training stability as synchronous RL methods. The feasibility of performing reinforcement learning training with micro-batches is theoretically demonstrated. Prompt-level asynchronous parallelism is employed to maximize the overlap between inference and training. A unified three-mode (policy, old policy, reference) architecture with identically distributed components is introduced, along with a shared-prompt attention mechanism that offers distinct advantages for long prompts and short responses. Experimental results demonstrate that the proposed framework achieves a three- to five-fold improvement in end-to-end performance over current mainstream RL training frameworks on the NPU platform. These results further support the equivalence in training effectiveness between the asynchronous and synchronous methods. Additionally, the decoupling of training and inference enables independent and flexible scaling, optimizing the balance between speed and device utilization. The decoupling of the training architecture and algorithm also ensures the proposed framework’s compatibility with other on-policy reinforcement learning algorithms, allowing them to benefit from the advantages of asynchronous training without requiring algorithmic modifications, nor ensuring the stability of modified algorithms.

## References

[Dao, 2023] Tri Dao. Flashattention-2: Faster attention with better parallelism and work partitioning. *arXiv preprint arXiv:2307.08691*, 2023.

[DeepSeek-AI, 2025] DeepSeek-AI. Deepseek-r1: Incentivizing reasoning capability in llms via reinforcement learning, 2025.

[Feng *et al.*, 2025] Laingjun Feng, Chenyi Pan, Xinjie Guo, Fei Mei, Benzhe Ning, Jianxiang Zhang, Xinyang Liu, Beirong Zhou, Zeng Shu, Chang Liu, Guang Yang, Zhenyu Han, Jiangben Wang, and Bo Wang. Mindspeed rl: Distributed dataflow for scalable and efficient rl training on ascend npu cluster, 2025.

[Fu *et al.*, 2025] Wei Fu, Jiaxuan Gao, Xujie Shen, Chen Zhu, Zhiyu Mei, Chuyi He, Shusheng Xu, Guo Wei, Jun Mei, Jiashu Wang, Tongkai Yang, Binhang Yuan, and Yi Wu. Areal: A large-scale asynchronous reinforcement learning system for language reasoning, 2025.

[Guo *et al.*, 2025] Daya Guo, Dejian Yang, Haowei Zhang, Junxiao Song, Peiyi Wang, Qihao Zhu, Runxin Xu, Ruoyu Zhang, Shirong Ma, Xiao Bi, et al. Deepseek-r1 incentivizes reasoning in llms through reinforcement learning. *Nature*, 645(8081):633–638, 2025.

[Hu *et al.*, 2024] Jian Hu, Xibin Wu, Zilin Zhu, Xianyu, Weixun Wang, Dehao Zhang, and Yu Cao. Openrlhf: An easy-to-use, scalable and high-performance rlhf framework. *arXiv preprint arXiv:2405.11143*, 2024.

[Hugging Face, 2025] Hugging Face. Open r1: A fully open reproduction of deepseek-r1, January 2025.

[Kwon *et al.*, 2023] Woosuk Kwon, Zhuohan Li, Siyuan Zhuang, Ying Sheng, Lianmin Zheng, Cody Hao Yu, Joseph E. Gonzalez, Hao Zhang, and Ion Stoica. Efficient memory management for large language model serving with pagedattention. In *Proceedings of the ACM SIGOPS 29th Symposium on Operating Systems Principles*, 2023.

[Lu *et al.*, 2025] Han Lu, Zichen Liu, Shaopan Xiong, Yancheng He, Wei Gao, Yanan Wu, Weixun Wang, Jiaashun Liu, Yang Li, Haizhou Zhao, Ju Huang, Siran Yang, Xiaoyang Li, Yijia Luo, Zihe Liu, Ling Pan, Junchi Yan, Wei Wang, Wenbo Su, Jiamang Wang, Lin Qu, and Bo Zheng. Part ii: Roll flash – accelerating rlrv and agentic training with asynchrony, 2025.

[Luo and others, 2025] Michael Luo et al. Deepscaler: Surpassing o1-preview with a 1.5b model by scaling rl. <https://tinyurl.com/deepscaler-2025>, 2025. Notion Blog.

[Noukhovitch *et al.*, 2024] Michael Noukhovitch, Shengyi Huang, Sophie Xhonneux, Arian Hosseini, Rishabh Agarwal, and Aaron Courville. Asynchronous rlhf: Faster and more efficient off-policy rl for language models. *arXiv preprint arXiv:2410.18252*, 2024.

[Rasley *et al.*, 2020] Jeff Rasley, Samyam Rajbhandari, Olatunji Ruwase, and Yuxiong He. Deepspeed: System optimizations enable training deep learning models with over 100 billion parameters. In *Proceedings of the 26th ACM SIGKDD international conference on knowledge discovery & data mining*, pages 3505–3506, 2020.

[Schulman *et al.*, 2017] John Schulman, Filip Wolski, Profulla Dhariwal, Alec Radford, and Oleg Klimov. Proximal policy optimization algorithms. *arXiv preprint arXiv:1707.06347*, 2017.

[Sheng *et al.*, 2024] Guangming Sheng, Chi Zhang, Zilingfeng Ye, Xibin Wu, Wang Zhang, Ru Zhang, Yanghua Peng, Haibin Lin, and Chuan Wu. Hybridflow: A flexible and efficient rlhf framework. *arXiv preprint arXiv:2409.19256*, 2024.

[Shoeybi *et al.*, 2019] Mohammad Shoeybi, Mostafa Patwary, Raul Puri, Patrick LeGresley, Jared Casper, and Bryan Catanzaro. Megatron-lm: Training multi-billion parameter language models using model parallelism. *arXiv preprint arXiv:1909.08053*, 2019.

[Team, 2025] Qwen Team. Qwen3 technical report, 2025.

[Wei *et al.*, 2022] Jason Wei, Xuezhi Wang, Dale Schuurmans, Maarten Bosma, Fei Xia, Ed Chi, Quoc V Le, Denny Zhou, et al. Chain-of-thought prompting elicits reasoning in large language models. *Advances in neural information processing systems*, 35:24824–24837, 2022.

[Yao *et al.*, 2023] Zhewei Yao, Reza Yazdani Aminabadi, Olatunji Ruwase, Samyam Rajbhandari, Xiaoxia Wu, Ammar Ahmad Awan, Jeff Rasley, Minjia Zhang, Conglong Li, Connor Holmes, Zhongzhu Zhou, Michael Wyatt, Molly Smith, Lev Kurilenko, Heyang Qin, Masahiro Tanaka, Shuai Che, Shuaiwen Leon Song, and Yuxiong He. DeepSpeed-Chat: Easy, Fast and Affordable RLHF Training of ChatGPT-like Models at All Scales. *arXiv preprint arXiv:2308.01320*, 2023.

[Zhang and Math-AI, 2024] Yifan Zhang and Team Math-AI. American invitational mathematics examination (aime) 2024, 2024.